



1 **Enhanced Terrestrial Runoff during Oceanic Anoxic Event 2 on the North** 2 **Carolina Coastal Plain, USA**

3 Christopher M. Lowery¹, Jean M. Self-Trail², Craig D. Barrie³

4 ¹University of Texas Institute for Geophysics, Austin, TX, USA

5 ²United States Geological Survey, Reston, VA, USA

6 ³GeoMark, LTD, Houston, TX, USA

7 *Correspondence to:* Chris Lowery cmlowery@utexas.edu

8 **Abstract**

9 A global increase in the strength of the hydrologic cycle drove an increase in flux of terrigenous
10 sediments into the ocean during the Cenomanian-Turonian Oceanic Anoxic Event 2 (OAE2) and was an
11 important mechanism driving nutrient enrichment and thus organic carbon burial. This global change is
12 primarily known from isotopic records, but global average data don't tell us anything about changes at
13 any particular location; such reconstructions of local terrigenous flux can help us understand the role of
14 regional shifts in precipitation in driving these global trends. The North Atlantic basin was one of the
15 epicenters of enhanced organic carbon burial during OAE2, and so constraining terrigenous flux is
16 particularly important in this region; however, few local records exist. Here, we present two new OAE2
17 records from the Atlantic Coastal Plain of North Carolina, USA, recognized with calcareous
18 nannoplankton biostratigraphy and organic carbon isotopes. We use carbon/nitrogen ratios to constrain
19 the relative contribution of marine and terrestrial organic matter; in both cores we find elevated
20 contribution from vascular plants beginning just before OAE2 and continuing through the event,
21 indicating a locally strengthened hydrologic cycle. Terrigenous flux decreased during the brief change in
22 carbon isotope values known as the Plenium carbon isotope excursion, and then increase and remain
23 elevated through the latter part of OAE2. TOC values reveal relatively low organic carbon burial in the
24 inner shelf, in contrast to black shales known from the open ocean. Organic carbon content on the shelf
25 appears to increase in the offshore direction, highlighting the need for cores from the middle and outer
26 shelf.



27 **1 Introduction**

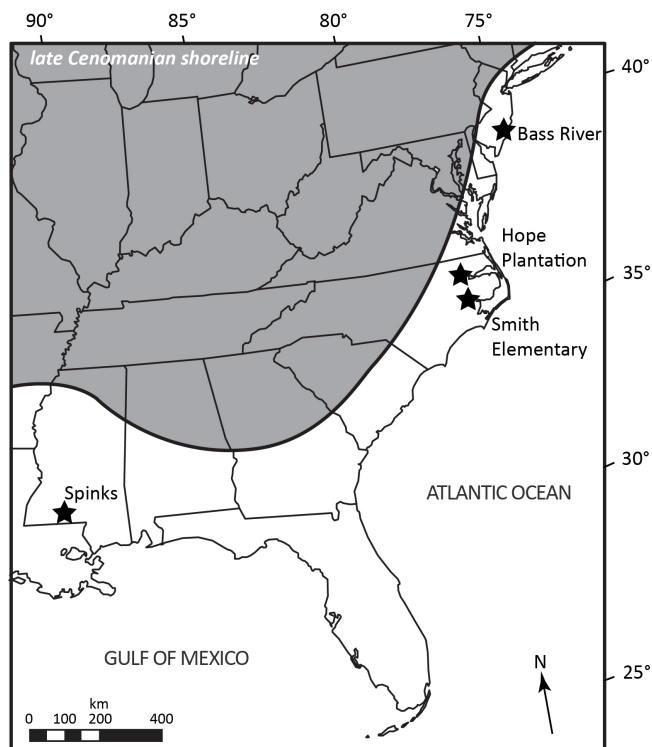
28 The Cretaceous was characterized by intermittent periods of enhanced organic carbon burial
29 linked to widespread black shale deposition and anoxia, termed Oceanic Anoxic Events (OAEs;
30 Schlanger and Jenkyns, 1976; Jenkyns 2010). Although OAEs were originally defined by the widespread
31 occurrence of black shales (Schlanger and Jenkyns, 1976) they were soon found to be associated with
32 positive carbon isotope excursions driven by the excess global burial of organic carbon and representing a
33 perturbation of the global carbon cycle (Scholle and Arthur, 1980; Arthur et al., 1987; Jenkyns, 2010;
34 Owens et al., 2017). OAEs eventually became linked with the emplacement of large igneous provinces
35 (Tarduno et al., 1991; Whitechurch et al., 1992; Leckie et al., 2002; Snow et al., 2005; Turgeon and
36 Creaser, 2008; Monteiro et al., 2012; McAnena et al., 2013), suggesting a causal mechanism for enhanced
37 organic carbon burial. In the case of the Cenomanian-Turonian OAE2, the emplacement of the Caribbean
38 Large Igneous Province (e.g., Snow et al., 2005) is associated with significant warming (e.g., Friedrich et
39 al., 2012) and resulted in a strengthening of the hydrological cycle and an increase in the flux of nutrients
40 to the oceans (Blätter et al., 2011; Pogge von Strandmann et al., 2013).

41 Carbon isotopes reveal global changes in organic carbon burial rates but don't tell us anything
42 about where that organic matter was buried. This is important because local organic matter enrichment
43 can vary significantly in both timing (e.g., Tsikos et al., 2004) and magnitude (e.g., Owens et al., 2018)
44 during an OAE. Similarly, the calcium isotope proxy used by Blätter et al. (2011) and the lithium isotope
45 proxy used by Pogge von Strandmann et al. (2013) to determine changes in global terrigenous flux to the
46 oceans don't tell us anything about local patterns of terrigenous runoff. Presumably, like organic carbon
47 burial, the hydrologic cycle did not increase uniformly, but instead some regions experienced a greater
48 change than others. Unfortunately, few local records of changes in the hydrologic cycle during OAE2
49 have been documented. Van Helmond et al. (2014) used palynological and biomarker data from the Bass
50 River core (Ocean Drilling Program Site 174X) on the coastal plain of New Jersey, USA, to document
51 local warming associated with enhanced contribution of terrestrial organic matter during OAE2. While



52 this result clearly indicates a stronger hydrologic cycle during OAE2, it only represents a single locality.
53 Similar work from Wunstorf, Germany, in the Lower Saxony Basin, reveals a clear association between
54 terrigenous flux (measured by palynology and biomarker data) and black shale development, but this
55 association isn't limited to OAE2, with additional intervals of elevated terrigenous input and black shale
56 deposition continuing after the end of the carbon isotope excursion (van Helmond et al., 2015). In the
57 Western Interior Seaway of North America, increases in kaolinite (a clay mineral formed in wet, humid
58 environments) during OAE2 may be the result of wetter conditions, but these trends may also be caused
59 by shifting sediment source areas (Leckie et al., 1998). Overall, these existing records paint an incomplete
60 picture.

61 To fully understand these trends, therefore, it is essential to develop similar datasets from
62 additional localities. Such work will allow a more geographically complete understanding of changes in
63 precipitation during OAE2 and thus provide a window into the mechanisms which drove hydroclimate
64 during the hottest part of the Cretaceous greenhouse. Here, we present two new OAE2 sections from
65 cores drilled by the United States Geological Survey (USGS) on the Coastal Plain of North Carolina, on
66 the Atlantic margin of North America (Figure 1). We use organic carbon isotopes and calcareous
67 nannoplankton biostratigraphy to identify the OAE2 interval and organic carbon/nitrogen (C/N) ratios to
68 detect changes in terrigenous flux. These cores are only the second and third OAE2 intervals described on
69 the Atlantic Coastal Plain after the Bass River core (Bowman and Bralower, 2005; van Helmond et al.,
70 2014) and thus also provide important context of the response of the inner shelf to OAE2, filling in an
71 important gap in an important region (e.g., Owens et al., 2018) during this well-studied time interval.



72

73 **Figure 1.** Map of southeastern North America showing approximate late Cenomanian shoreline (land = grey) and
74 the location of the cores discussed in this study. Shoreline position after Slattery et al. (2015) and Snedden et al.
75 (2015).

76 **2 Geologic Setting**

77 Cenomanian and Turonian sediments of the Atlantic Coastal Plain of the United States (Figure 1)
78 are part of a sequence of strata that accumulated since the rifting of the Atlantic began in the Early
79 Jurassic. However, study of the marine units of these sediments is difficult due to the absence of outcrops
80 of this age and environment on the Coastal Plain (Sohl and Owens, 1991). Thus, their study is restricted
81 to the limited number of cores and/or cuttings available and regional interpretations are often based on
82 geophysical data obtained from water wells and scattered oil and gas test wells.

83 To the south, initial subsurface work in Florida and Georgia followed the nomenclature of the
84 Gulf Coastal Plain. Sediments from Georgia were variously attributed to the Cenomanian Woodbine



85 Formation, the Cenomanian/Turonian Eagle Ford Formation, and the Cenomanian/Turonian Tuscaloosa
86 Formation (Applin and Applin, 1944; Richards, 1945). Applin and Applin (1947) later introduced the
87 name Atkinson Formation, with three unnamed members (upper, middle, and lower) for marine rocks in
88 the subsurface of southern Alabama, southern Georgia, and northern Florida. They correlated the lower
89 member of the Atkinson to nonmarine sands and shales of the Coastal Plain of Georgia, which they
90 considered to be Cenomanian in age, and the middle member of the Atkinson to the Tuscaloosa Marine
91 Shale, which they considered to be Cenomanian/Turonian in age (Applin and Applin, 1967).

92 Early work in South Carolina by Cooke (1936), Dorf (1952), and Heron (1958) considered
93 outcrops of the Middendorf Formation to be Cenomanian in age, based largely on stratigraphic position
94 and on long-ranging pollen and/or mollusks. Similarly, outcrops of the largely non-marine Cape Fear
95 Formation in North Carolina were attributed to the Cenomanian (Stephenson, 1912; Cooke, 1936).
96 Outcrops thought to be Turonian in age from both states were largely assigned to the Black Creek
97 Formation.

98 A shift in thinking regarding stratigraphic nomenclature was spurred by examination of sediments
99 from the Clubhouse Crossroads #1 core by Hazel et al. (1977) who found clear evidence of true
100 Cenomanian/Turonian marine rocks that indicated outcrops in the region must be different ages.
101 Calcareous nannofossils and foraminifera of Cenomanian and Turonian age were identified (Hazel et al.,
102 1977; Hattner and Wise, 1980; Valentine, 1984) and correlated with cuttings from the Fripp Island well
103 (Valentine, 1984) to provide better understanding of the subsurface geology of the region. In North
104 Carolina, Zarra (1989) reinterpreted the work of Spangler (1950) using both foraminifera and sequence
105 stratigraphic concepts, positively identifying Cenomanian and Turonian sediments from the Esso #1 core
106 and from cuttings of the Mobile #1, Mobile #2, Mobile #3, and Marshall Collins #1 test wells. He used
107 sedimentary and well log analysis to identify marginal marine and inner shelf facies in the lower/middle
108 Cenomanian and middle Turonian, with a highstand in the upper Cenomanian. These cores all contained a



109 diverse assemblage of planktic foraminifera, including species belonging to *Rotalipora*,
110 *Praeglobotruncana*, *Dicarinella*, *Whiteinella*, and *Guembelitra* (Zarra et al., 1989).

111 This reevaluation ultimately resulted in the formal designation of the Cenomanian/Turonian
112 Clubhouse Formation (Gohn, 1992) in the Clubhouse Crossroads core. At the type locality, the
113 Clubhouse Formation consists of gray to gray-green, fine- to medium- grained micaceous sands with
114 flaser to lenticular bedding and common bioturbation. Sequence stratigraphic analysis suggests that
115 deposition occurred in a shelf environment proximal to the shoreline and that these sediments represent
116 latest Cenomanian/earliest Turonian sea level rise prior to the early Turonian highstand event (Aleman
117 Gonzalez et al., 2020). The subsurface extent of this formation has now been documented across much of
118 South and North Carolina (Weems et al. 2007; Weems et al., 2019; Aleman Gonzalez et al., 2020).

119 To the north, published documentation of marine Cenomanian/Turonian sediments from the mid-
120 Atlantic region appears to be limited to the E.G. Taylor No. 1-G well on the eastern shore of Virginia.
121 Valentine (1984) reports the presence of *Rotalipora greenhornensis*, which went extinct in the latest
122 Cenomanian, from one sample at 1520 ft.

123 Cenomanian/Turonian sediments of the northeast Atlantic Coastal Plain consist of the subsurface
124 Bass River Formation and its correlative updip equivalent, the Raritan Formation in Maryland, New
125 Jersey, and Delaware. The Bass River Formation is herein considered to be correlative with the
126 Clubhouse Formation of the southeastern Atlantic Coastal Plain. The Bass River Formation was first
127 described by Petters (1976) from the TC16 well in Bass River Township, New Jersey. It was named as
128 the fully marine equivalent of the Raritan Formation and is differentiated by its common shell material
129 and deeper water depositional environment (Miller et al., 1998). The Bass River Formation has variously
130 been assigned a late Cenomanian to early Turonian age in a variety of cores and wells based on
131 foraminifera (Petters, 1976, 1977; Miller et al., 1998; Sikora and Olsson, 1991), calcareous nannofossils
132 (Valentine, 1984; Miller et al., 1998; Self-Trail and Bybell, 1995), and ostracodes (Gohn, 1995). Miller



133 et al., (2004) document that the Bass River Formation was deposited predominantly in inner neritic to
134 middle neritic paleodepths.

135 **3 Methods**

136 **3.1 Study Sites**

137 The Hope Plantation core (BE-110-2004) was drilled by the USGS in April to May, 2004 in
138 Bertie County, North Carolina, on the property of Hope Plantation (36.0323°N; 78.0192°W) (Figure 1).
139 The hole was drilled as a stratigraphic test for Atlantic Coastal Plain aquifers, and was continuously cored
140 to a total depth of 333.6 m (1094.5 ft) below land surface. A suite of wireline logs, including natural
141 gamma ray and resistivity logs, were collected at the completion of drilling. Preliminary work placed the
142 marine Cenomanian/Turonian boundary interval between approximately 182.8-228.6 m (600-750 ft). A
143 summary of the general stratigraphy, downhole logging, and core images can be found in Weems et al.
144 (2007).

145 The Smith Elementary School core (CR-675) was drilled by the USGS in February and March,
146 2006 in Craven County, NC, on the grounds of the nominate school (35.2511°N; 77.2903°W) (Figure 1).
147 It was continuously cored to a total depth of 323.1 m (1094.5 ft) . Difficulties with the wireline tools and
148 borehole stability limited the collection of geophysical logs, and only a partial natural gamma ray log
149 exists for the Clubhouse Formation for this core. There the marine interval that spans the
150 Cenomanian/Turonian boundary is between 288.3-323.1 m (945.9-1060.0 ft). Both cores are stored at the
151 North Carolina Geological Survey Coastal Plain core storage facility in Raleigh, NC, where we sampled
152 them in May, 2019.

153 **3.2 Calcareous Nannofossils**

154 One hundred ten samples from Hope Plantation and 84 samples from Smith Elementary School
155 were examined for calcareous nannofossil content. Samples were taken from the central portion of broken
156 core in order to avoid contamination from drilling fluid. Smear slides were prepared using the standard



157 techniques of Bown and Young (1998) in samples with low total organic carbon (TOC); samples with
158 increased TOC were prepared using the techniques of Shamrock et al. (2015) and Shamrock and Self-
159 Trail (2016). Coverslips were affixed using Norland Optical Adhesive 61. Calcareous nannofossils were
160 examined using a Zeiss Axioplan 2 transmitted light microscope at 1250x magnification under crossed
161 polarized light. Light microscope images were taken using a Powershot G4 camera with a Zeiss phototube
162 adaptor. Specimens were identified to the species level and correlated to the zonation schemes of
163 Sissinghi (1977) and Burnett (1988), as modified by Corbett et al. (2014) for shelf settings.

164 **3.3 Foraminifera**

165 Ninety samples were prepared for examination of planktic and benthic foraminifera.
166 Approximately 15 grams of material were soaked in a mixture of peroxide and borax for at least 24 hours,
167 washed over a 63 μm sieve, dried overnight in an oven, and then examined for microfossils using a Zeiss
168 Discovery V8 light microscope.

169 **3.4 TOC, C/N, and $\delta^{13}\text{C}$**

170 Core samples were analyzed for both their organic carbon isotope signature ($\delta^{13}\text{C}$ VPDB) and
171 elemental composition (%C and %N). To remove inorganic carbon content all of the material to be
172 analyzed was initially washed with hydrochloric (HCl) acid. There is was no anticipated inorganic
173 nitrogen content in the samples. All of the samples were analyzed on an elemental vario ISOTOPE select
174 cube elemental analyzer (EA) connected to a VisION isotope ratio mass spectrometer (IRMS). The EA
175 system follows dumas combustion and both generates and separates the gasses used for elemental
176 composition determination and then releases the gas to the IRMS for isotopic determination. The
177 elemental results were calibrated against a known sulfanilamide standard and the precision of the results
178 is +/-0.1% or better. The carbon isotope results were calibrated against four known reference standards
179 which cover the range of isotopic signatures expected in organic material (-15‰ to -35‰). All of the



180 isotopic results are reported in per mil (‰) relative to VPDB and the precision of the results is +/-0.1‰ or
181 better.

182 **4 Results**

183 **4.1 Lithology**

184 Qualitative core descriptions are summarized below and in Figures 2 and 3. Broad
185 paleoenvironmental interpretations are based on lithology, paleontology, and stratigraphic relationships.
186 Benthic foraminifera, which are powerful tools to determine paleoenvironment in marginal marine
187 settings (e.g., Tibert and Leckie, 2004), are unfortunately absent here due to poor preservation (see
188 section 4.2 below). In both cores we recognize two informal members of the Clubhouse Formation: a
189 marine lower member characterized by bivalves, calcareous nannoplankton, finer grained sediments,
190 thinner beds, and sedimentary features common to inner neritic environments; and a less marine upper
191 member characterized by coarser grainsize, thicker beds, and woody plant debris instead of calcareous
192 marine fossils, indicating deposition in a delta front or distributary environment.

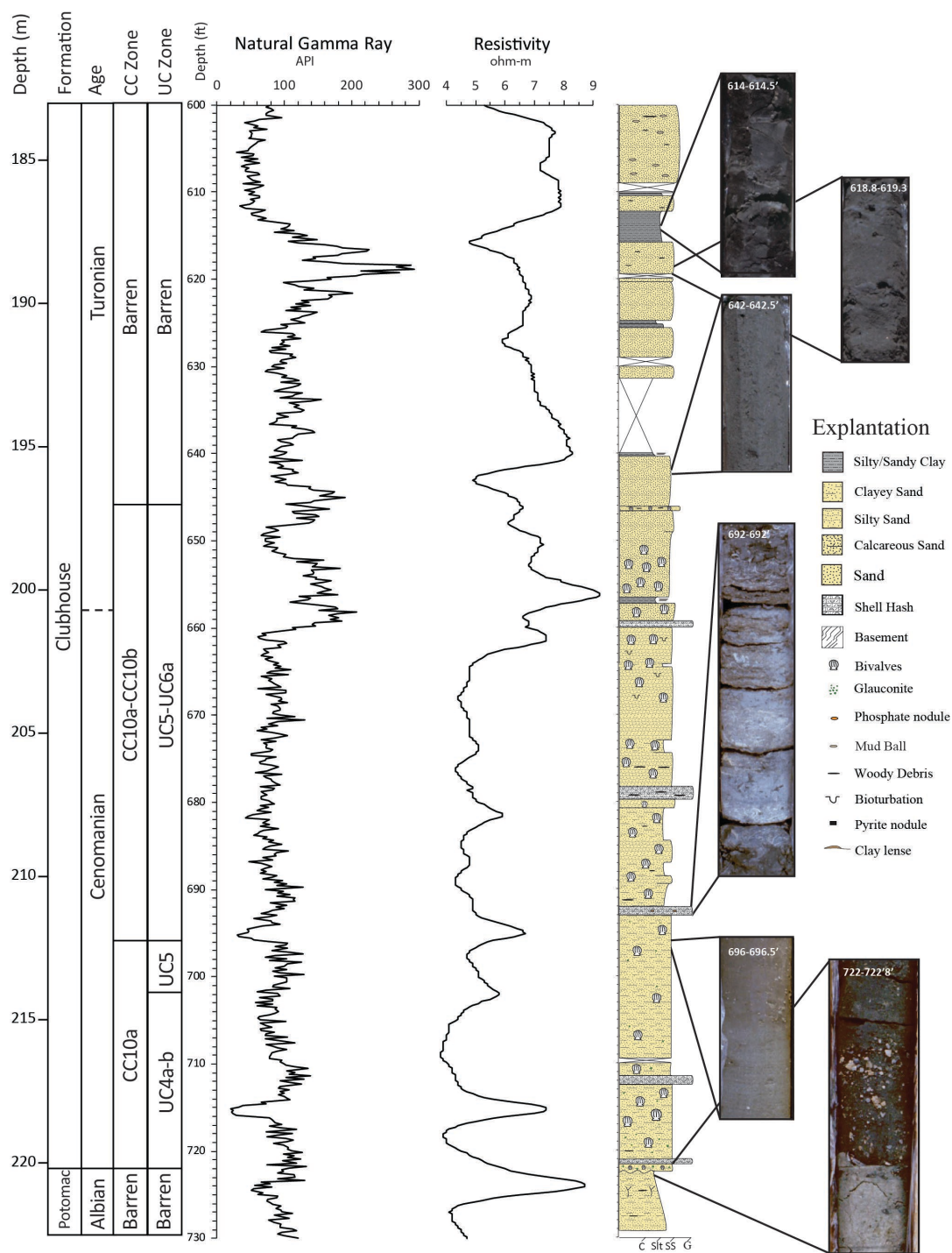


Figure 2. Stratigraphic column for Hope Plantation Core with CC and UC calcareous nannoplankton biozones, natural gamma ray and resistivity logs, and representative core images. C = clay; Slt = silt; SS = sand; G = gravel.



194 The Clubhouse Formation in the Hope Plantation Core (Figure 2) was penetrated between 174.3
195 m and 220.2 m below the surface. It is underlain by the floodplain paleosols of the Aptian Potomac Group
196 (Thornberg, 2008) and is overlain by undifferentiated sands and muds questionably assigned to the Cape
197 Fear Formation (Weems et al., 2007). The Clubhouse Formation is primarily composed of clayey and
198 silty sands punctuated by a few discrete skeletal limestones. The whole unit coarsens upward from clayey
199 sands (from the base of the formation to about 210.0 m) to silty sands (from about 210.0 m to about 201.2
200 m) to cleaner sands (from about 201.2 to the top of the formation). This upper change corresponds with a
201 clear change in gamma ray log response that characterizes most of the informal non-marine member. The
202 informal marine member extends from the base of the unit to the highest common occurrence of bivalves
203 and calcareous nannoplankton, around 196.9 m. Glauconite occurs from the base of the unit up to about
204 211.2 m. Four decimeter-scale skeletal limestones composed of broken bivalves occur roughly evenly
205 spaced through this informal member. Widely scattered woody debris is found between 210.6 m and
206 206.0 m. Clear bioturbation is rare but is evident between 203.6 and 201.2 m, just below the shift in
207 lithology from silty sand to cleaner sand. Bivalves occur throughout the informal marine member in
208 varying abundance from the base of the core. The non-informal marine member of the Clubhouse
209 Formation is characterized by massive sand interbedded with variably thick beds of massive silty clay, an
210 increasing abundance of woody debris above 189.0 m, and the occurrence of cm-scale mud balls above
211 185.6 m. A single thin bed containing bivalves occurs at 196.9 m. Given the more terrestrial features,
212 cleaner sands, and thin clay interbeds of the upper informal member of the Clubhouse Formation we
213 suggest that these sediments were deposited in a marginal marine environment such as a distributary
214 mouth bar or interdistributary bay system in the upper part of the Clubhouse Formation.



215

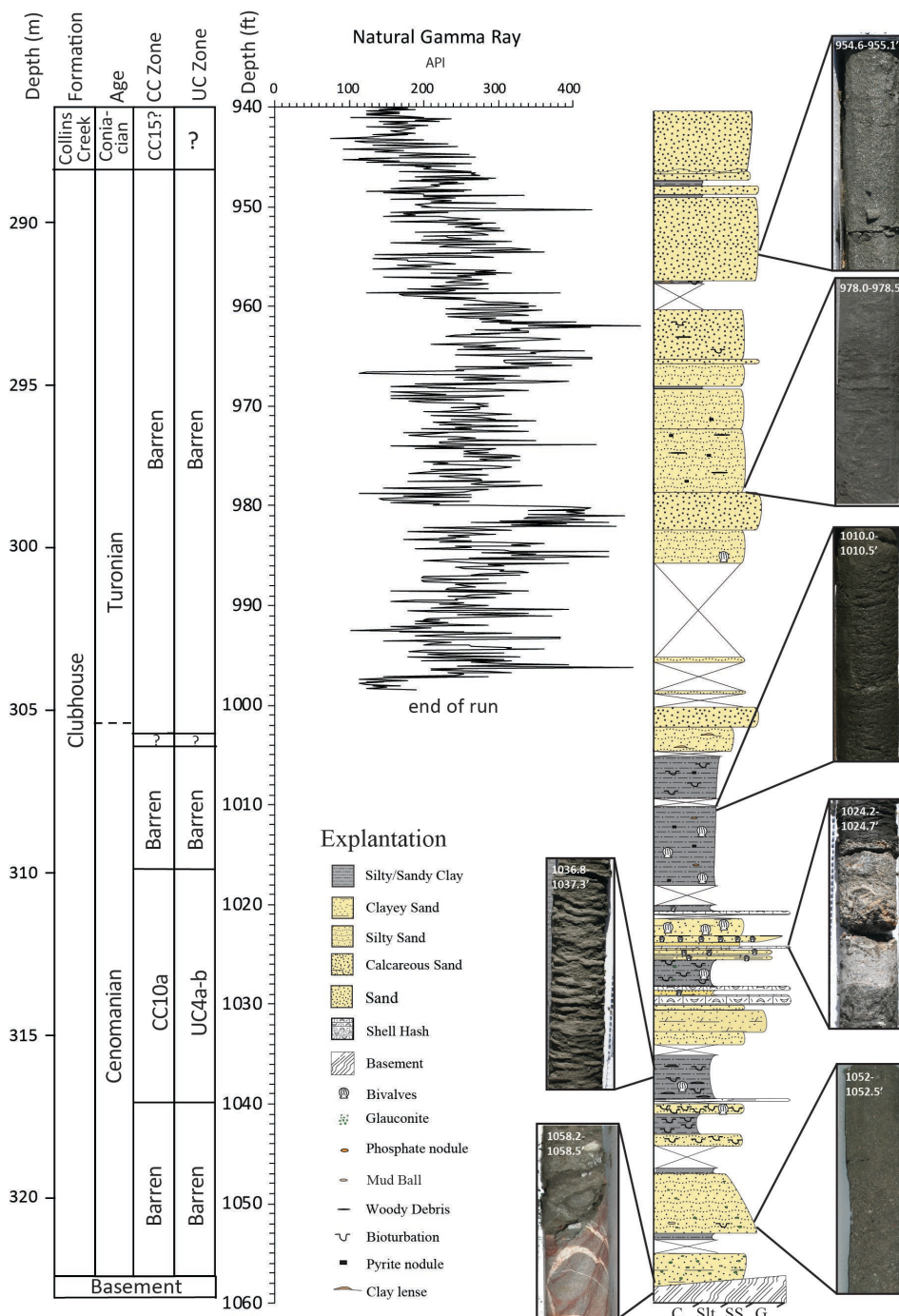


Figure 3. Stratigraphic column for the Smith Elementary School core, with CC and UC calcareous nannoplankton biozones, natural gamma ray log, and representative core images.



216 In the Smith Elementary core (Figure 3), the Clubhouse Formation occurs between 288.5 m and
217 322.7 m. Its basal contact with underlying gneiss is marked by a fault, with an angular contact ($\sim 45^\circ$ to
218 vertical in the core) and slickensides (Weems et al., 2007). This fault is overlain by ~ 15 cm thick interval
219 of dolomitic sand. The lithology of the Clubhouse Formation in the Smith Elementary core is overall
220 more fine-grained than that of the Hope Plantation, with a lower fining-upwards interval, muds and
221 limestones in the middle, and then coarsening upward to the unconformable upper contact with the
222 Santonian marginal marine Collins Creek Formation. The informal marine member of the Clubhouse
223 Formation in the Smith Elementary core (322.7–305.0 m) contains a more varied lithology than that of
224 the Hope Plantation core. The basal interval is a 2.6 m thick package of massive coarsening upward and
225 then fining upward clayey to silty glauconite-bearing sandstone separated by a thin silty claystone above a
226 ~ 35 cm core gap. Coring gaps of this scale are more common in the Smith Elementary core and are
227 associated with the contacts between sand and clay intervals. A single burrow occurs in the upper
228 sandstone bed, and glauconite decreases upsection. The next section is composed of bioturbated clay and
229 silty clay, with two ~ 30 cm thick silty sandstones with abundant burrows and rare bivalves. The upper
230 silty claystone contains thin clay lenses. This claystone is overlain by an interval of interbedded silty- to
231 clayey sandstone, skeletal limestones composed of broken bivalve debris, including one which has been
232 dolomitized, and a ~ 80 cm thick bioturbated silty claystone containing glauconite and bivalve shells. The
233 overlying interval is a 5.2 m thick silty claystone with planar bedding, phosphate nodules, pyrite, and
234 bivalve shells. The lower 3.4 m of this claystone is laminated with no visible bioturbation. Overall this
235 interval represents a fining upward sequence from sand to sandy silt to silty clay; the sandy clay contains
236 thin discrete beds of coarser material, include shell hash, possibly indicating deposition above storm wave
237 base before deepening to uniform silty clay representing deposition on the shelf below storm wave base at
238 the top of the informal marine member.

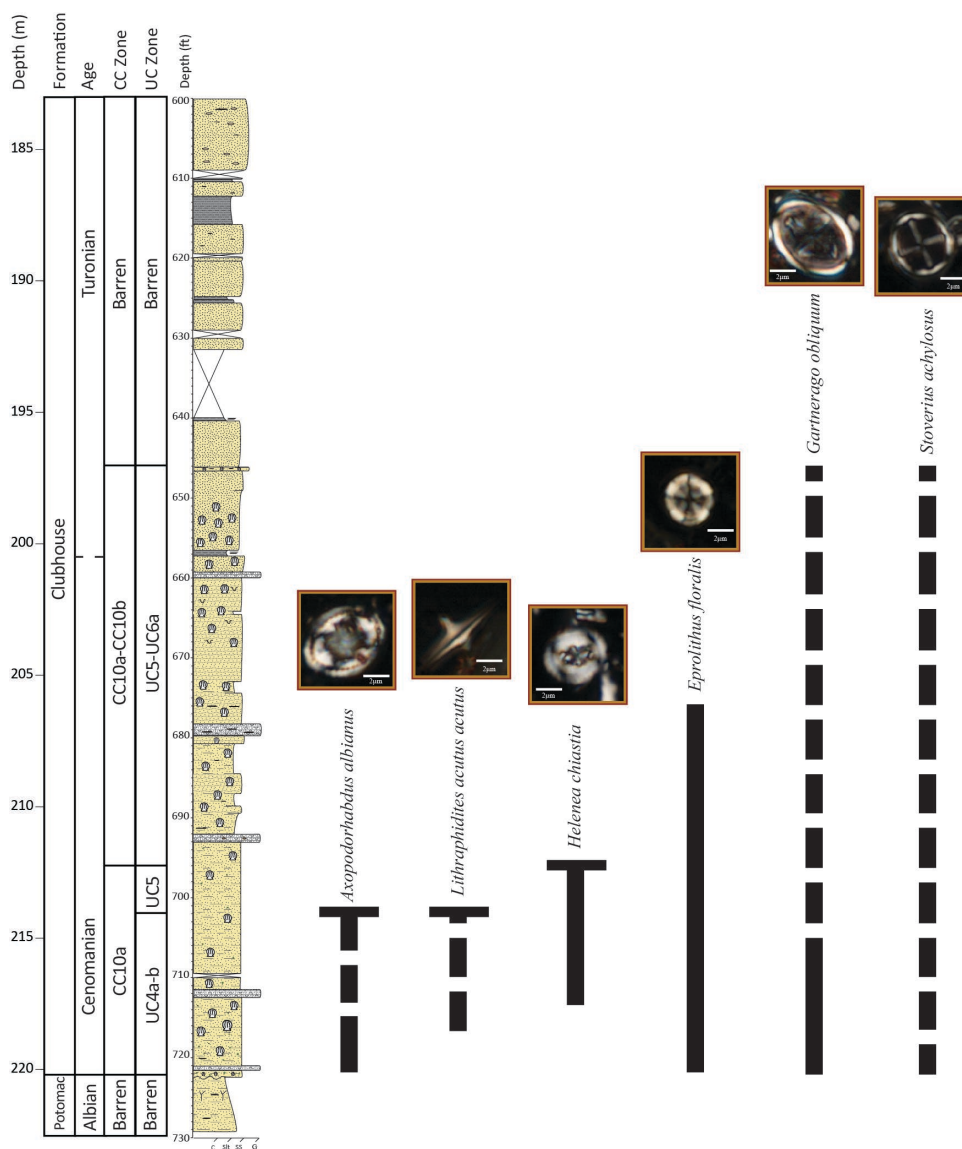
239 The informal non-marine member of the Clubhouse Formation in the Smith Elementary Core
240 (~ 305.0 -288.5 m) is composed of meter-scale beds of silty to well-sorted sandstone generally becoming



241 coarser up section, interbedded with centimeter scale beds of claystone. Some beds contain woody debris
242 and pyrite. A single bivalve occurs near the very base of the unit, and a few discrete burrows are observed
243 between 294 and 292 m. Flaser bedding occurs in a clay bed at 291.7 m. The overall coarse-grained
244 nature of these beds, and the alternating terrestrial and marine indicators lead us to interpret this interval
245 as being marginal marine, perhaps representing distributary mouth bars. The overlying contact with the
246 Collins Creek Formation is marked by a clear unconformity.

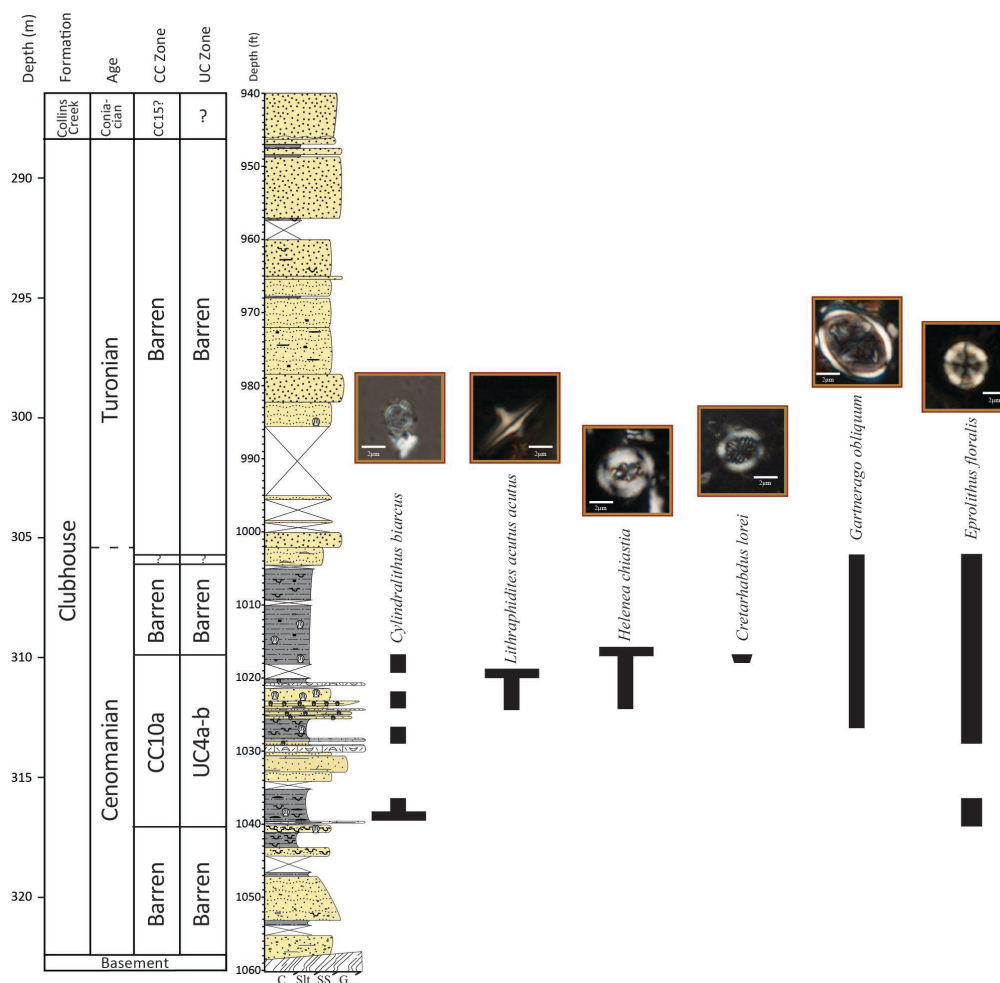
247 **4.2 Biostratigraphy**

248 Calcareous nannofossil assemblages are prevalent in the Hope Plantation core (Figure 4), with
249 abundances ranging from rare to common and preservation from good to poor; the top of the Clubhouse
250 Formation is barren (196.8-185.5 m) (Self-Trail et al., 2021). The basal Clubhouse is placed in the late
251 Cenomanian Zone UC4a-b of Burnett (1988) and Zone CC10a of Sissinghi (1977) based on the presence
252 of *Lithraphidites acutus*, whose highest occurrence (HO) at 214.0 m marks the top of Zone UC4b. The
253 absence of *Cretarhabdus loriei*, whose HO marks the top of UC4a, could be due to environmental
254 conditions, and thus sediments in this interval are lumped together into a combined zone (UC4a-b). A
255 condensed (or truncated) interval from the top of *L. acutus* to the HO of *Helenea chiastia* at 212.9 m is
256 placed in Zone UC5 (undifferentiated) and is latest Cenomanian in age. It is unclear from nannoplankton
257 data alone whether the HO of *H. chiastia* is the true extinction of this taxon (and thus this level marks the
258 latest Cenomanian) or if this absence of this species above the level is the result of poor preservation
259 and/or ecological exclusion from the inner shelf as increased terrigenous flux made the waters less
260 welcoming to marine nannoplankton. We favor the latter explanation, because the sample immediately
261 above the highest *H. chiastia* is barren, and marks the beginning of an interval characterized by poor
262 preservation and occasional barren samples. This interval, from 212.1-197.0 m, is placed in zones UC5-
263 UC6a and CC10a-CC10b based on the absence of both *H. chiastia* and *Eprolithus moratus*, whose lowest
264 occurrence (LO) defines the base of Zone UC6b. The Cenomanian/Turonian boundary is placed at 200.3
265 m based on carbon isotope data (see section 4.3.1, below).



266

267 **Figure 4.** Ranges of key calcareous nannoplankton species in the Hope Plantation Core. Dashed lines indicate
 268 sporadic occurrence.





278 b/Zone CC10a. The rare occurrence of poorly preserved calcareous nannofossils at 305.9 m suggest
279 continued placement in the Cenomanian or Turonian, but no diagnostic species were recovered, and thus
280 the Cenomanian/Turonian must once again be placed using carbon isotopes at 305.4 m (see section 4.3.1,
281 below). An unconformity at the top of the Clubhouse Formation (288.4 m) corresponds to a change from
282 a barren interval below to a Santonian assemblage of calcareous nannofossils above.

283 All samples examined for planktic and benthic foraminifera were entirely barren of whole
284 specimens. A few contained very rare fragments of both planktic and benthic foraminifera, indicating that
285 foraminifera were present in these sections but that they were subsequently dissolved, either in situ or in
286 the 17 years since the cores were drilled. This may be in part due to the relatively organic-rich nature of
287 the sediments and to the presence of pyrite, both of which have been found to result in dissolution of
288 calcareous microfossils in cored sediments of the Atlantic Coastal Plain (Self-Trail and Seefelt, 2005;
289 Seefelt et al., 2015). However, the well-documented occurrence of planktic and benthic foraminifera in
290 more distal coastal plain cores (e.g., Valentine, 1982, 1984; Zarra, 1989; Gohn, 1992) bodes well for
291 future micropaleontological studies in this region.

292 **4.3 Geochemistry**

293 **4.3.1 Carbon Isotopes**

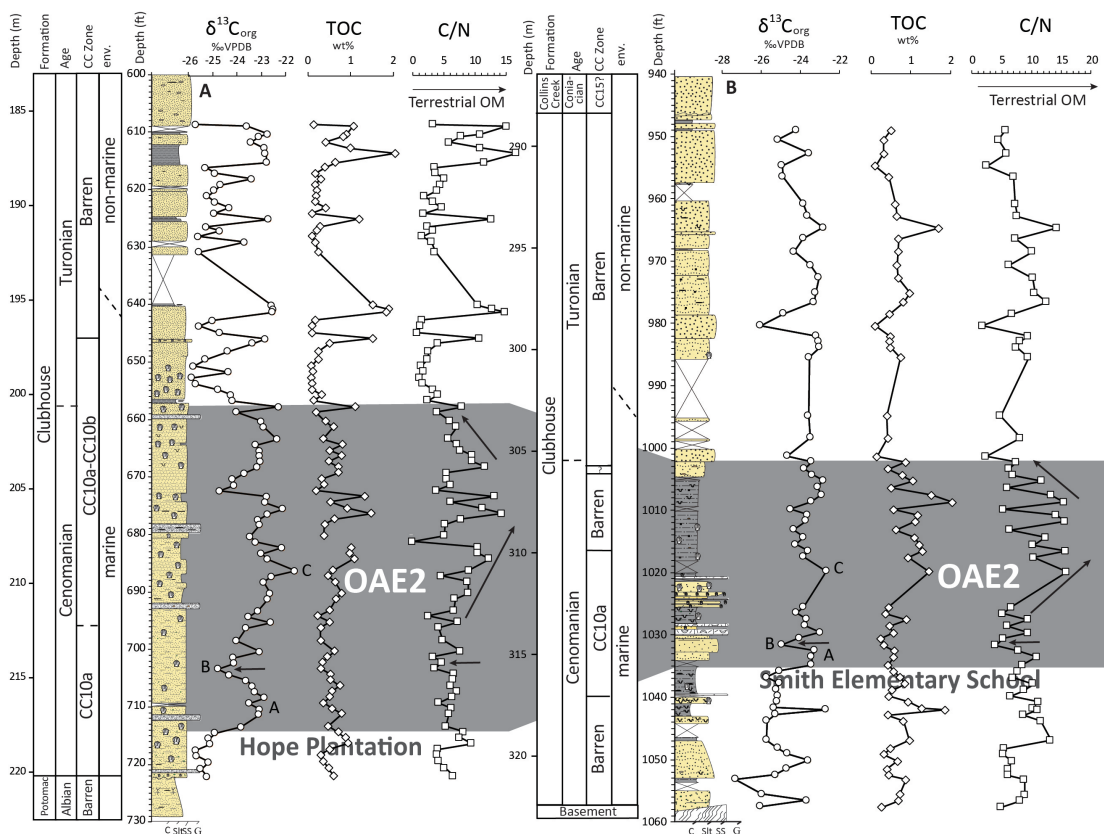
294 Organic carbon isotope ($\delta^{13}\text{C}$) data (Figure 6) in each core show clear positive excursions
295 associated with OAE2 in the marine interval of the Clubhouse Formation. Both isotope records display a
296 ~2‰ positive shift with the classic A-B-C structure of OAE2, with an initial excursion (A), a brief
297 recovery followed by a second peak (B) and a longer plateau with a small peak (C) first described by Pratt
298 and Threlkeld (1984) in the US Western Interior Seaway. The Hope Plantation core, which is
299 characterized by coarser grains and a more proximal environment, has a more expanded OAE2 interval (~
300 17.4 m) compared to the somewhat more distal Smith Elementary Core (~ 10.4 m). The termination of the



301 OAE2 carbon isotope excursion roughly corresponds with the Cenomanian-Turonian boundary (e.g.,
302 Kennedy et al., 2005) and has been used to define that level in our cores.

303 4.3.2 Total Organic Carbon

304 Total organic carbon data (Figure 6) reveals relatively low enrichment in organic carbon in the
305 Hope Plantation core, generally <1 weight percent (wt%) TOC except for a few discrete peaks associated
306 with woody debris. Average values are slightly higher during OAE2 (~0.6 wt%) compared to background
307 levels in the overlying interval (~0.4 wt%) but just barely. Values are slightly higher overall in the Smith
308 Elementary School core, particularly during OAE2, where the upper part of the event averages about 1.0
309 wt% TOC.



310



311 **Figure 6.** Geochemical data from the Hope Plantation (left) and Smith Elementary School (right) cores
312 plotted against stratigraphic columns for each. Grey shaded area represents the OAE2 interval in each
313 core. Letters A-B-C labels on carbon isotope ($\delta^{13}C$) curve correspond to named points of the OAE carbon
314 isotope excursion. TOC = total organic carbon; C/N = carbon/nitrogen ratio. Arrows indicate brief
315 reduction in C/N ratio coincident with the Plenus isotope excursion (“B” on the $\delta^{13}C$ plot) and broad
316 increase in values during the main part of the $\delta^{13}C$ excursion. Note slight change in depth scale between
317 the two cores, as the studied interval in Smith Elementary is 10 ft (3.1 m) thicker than Hope Plantation.

318 4.3.3 Organic Carbon/Nitrogen Ratios

319 The ratio of total organic carbon to total nitrogen is a common proxy for the relative contributions
320 of algae and land plants to sedimentary organic matter (e.g., Meyers, 1994, 1997, 2003). Due to
321 differences in their composition (e.g., the abundance of cellulose in land plants) vascular plants tend to
322 have C/N ratios of 20 or greater, while algae have C/N ratios of 4-10 (Meyers, 1994). Changes in C/N
323 ratio in marine settings therefore reflect changes in the relative contribution of terrigenous organic matter
324 to offshore areas. This can be used to reconstruct changes in the hydrologic cycle, with increased C/N
325 ratios indicating a higher flux of terrestrial organic matter due to enhanced weathering (Meyers, 2003).
326 Sediments with low TOC (<0.3 wt%) can cause problems for C/N interpretations because in such settings
327 the proportion of inorganic nitrogen can be high enough to artificially depress the data, suggesting more
328 marine organic matter than is really there (Meyers et al., 1997); our data is consistently above 0.5 wt%
329 TOC so this is not a concern (see section 4.3.2, above).

330 C/N ratios in both cores are elevated during OAE2, indicating enhanced contribution of terrestrial
331 organic matter driven by a strengthened hydrologic cycle (Figure 6). An increase in C/N precedes the
332 onset of OAE2 by at least a meter in both cores, and the shape of the C/N ratio curves are similar. Values
333 are slightly elevated prior to and through the start of the event and then decline coincident with the brief
334 recovery in carbon isotope values (the B part of the carbon isotope excursion). C/N values then recover
335 along with carbon isotope values, and become increasingly elevated during the latter phase of OAE2,
336 coincident with the long plateau of the carbon isotope excursion. In both cores there is some obvious



337 variability in the C/N ratios, particularly during the interval of the highest values later in the event.
338 Background values in both cores return to pre-excursion levels following the termination of OAE2,
339 although single samples contain occasionally elevated values. This probably reflects contributions of
340 discrete bits of woody plant debris, which occur sporadically through the upper (non-marine) interval of
341 the Clubhouse Formation.

342 **5 Discussion**

343 **5.1 Enhanced Hydrologic Cycle During OAE2**

344 Our data indicate a strengthened hydrologic cycle in southeastern North America preceding the
345 start of OAE2 and continuing through the event, in agreement from the data from van Helmond et al.
346 (2014) some 500 km to the north. Palynological data from New Jersey agree with our bulk geochemical
347 data in showing highest terrigenous flux during the latter part of the OAE2 isotope excursion. The pre-
348 event increase in terrigenous flux is an interesting parallel to records of pre-event global oxygen
349 drawdown based on thallium isotopes (Ostrander et al., 2017), suggesting a link between weathering flux
350 and deoxygenation, likely via enhanced delivery of nutrients to the oceans. Additionally, a drop in C/N
351 ratio in both of our core records during the carbon isotope minimum referred to as the Plenus carbon
352 isotope excursion (O'Connor et al., 2019) indicate relatively drier conditions at this time, a phenomenon
353 also observed in New Jersey coincident with a decrease in temperatures (van Helmond et al., 2014). The
354 Plenus Cold Event was originally interpreted as a global cooling event (hence the name, e.g., Gale and
355 Christensen, 1996) caused by CO₂ drawdown resulting from high rates of organic carbon burial at the
356 onset of OAE2 (Erbacher et al., 2005; Jarvis et al., 2011; Hasegawa et al., 2013; Gale, 2019). However,
357 more detailed comparisons of temperature and carbon isotope records from a wide range of sites has
358 demonstrated that the timing and magnitude of cooling varies significantly by location (O'Connor et al.,
359 2019). Our results agree with those of van Helmond et al. (2014) that the carbon drawdown associated
360 with the Plenus interval resulted in a weaker hydrologic cycle and reduced terrigenous flux into the
361 oceans, at least along the east coast of North America.



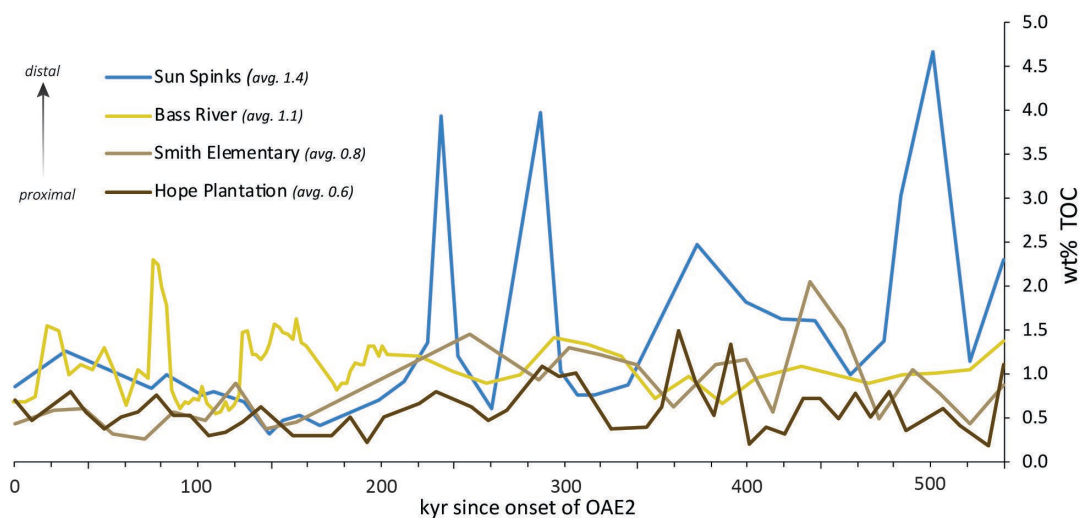
362 5.2 OAE2 on the eastern North American shelf

363 The Smith Elementary School and Hope Plantation cores represent the second and third records
364 of OAE2 on the US Atlantic Coastal Plain. As such, they provide important insight into a surprisingly
365 understudied region. In the modern ocean, about 85% of organic carbon burial occurs along continental
366 margins (e.g., Burdige, 2007). A survey of all known OAE2 localities with a complete carbon isotope
367 excursion and TOC data by Owens et al. (2018) found that there is a significant amount of “missing”
368 organic carbon when reconstructed organic carbon burial is compared to “expected” carbon burial based
369 on carbon isotope data. This was based on 170 sites which, with some extrapolation, represent just 13%
370 of total Cenomanian-Turonian ocean area, which meant that similar values had to be assumed for the rest
371 of the seafloor (Owens et al., 2018). OAE2 is perhaps the best studied event of the Cretaceous, but these
372 results suggest a clear need for additional sites to better constrain paleoceanographic and
373 paleoenvironmental changes during this event. By adding additional OAE2 sites on the Atlantic Coastal
374 Plain our results help to constrain the contribution of these areas to global carbon burial.

375 Van Helmond et al. (2014) point out that TOC is lower in the Bass River core than other OAE2
376 sections in the North Atlantic region, but our results indicate that Bass River is about average for inner
377 continental shelf deposits (Figure 7). Average TOC during OAE2 at Bass River is 1.1 wt% (van
378 Helmond, 2014); this is slightly higher than Smith Elementary (0.83 wt%) and Hope Plantation (0.63
379 wt%) and slightly lower than the next closest published shelf site to the southwest, the Sun Spinks core in
380 Mississippi (1.4 wt %, Lowery et al., 2017). Sequence stratigraphic analysis of Cenomanian/Turonian
381 sediments of the Clubhouse and Bass River formations show that these sediments represent maximum sea
382 level rise across the boundary on the Atlantic Coastal Plain (Aleman Gonzalez et al., 2020; Miller et al.,
383 2004). The location of the Hope Plantation core (lowest TOC values) higher on the inner paleoshelf
384 relative to Smith Elementary School and Bass River (higher TOC values) suggests that TOC wt% on the
385 shelf during OAE2 was, at least in part, a function of paleodepth. To be sure, these are certainly lower
386 than values found offshore in the open ocean or along upwelling margins in the eastern North Atlantic.



387 For example, Deep Sea Drilling Project Site 603, on the lower continental rise directly offshore of North
388 Carolina, has an average TOC of 5.4 wt % during OAE2 (Kuypers et al., 2004), while the upwelling-
389 prone region at Tarfaya, Morocco has an average TOC of 8.0 wt% (Kolonic et al., 2005).



390

391 **Figure 7.** Comparison of measured wt% TOC for the duration of OAE2 for the Sun Spinks core in Mississippi, Bass
392 River core in New Jersey, and the Smith Elementary School and Hope Plantation cores in North Carolina. Age
393 model based on the thickness of the OAE carbon isotope excursion and the orbitally-tuned duration of OAE2 at the
394 Global Stratotype Section and Point in Pueblo, CO (Sageman et al., 2006; Meyers et al., 2012) of 540 kyr, assuming
395 a constant sedimentation rate.

396 Sedimentation rate also plays an important role in organic carbon accumulation. While we don't
397 have dry bulk density measurements from these cores to calculate mass accumulation rates, we can
398 approximate using reasonable values for organic-rich silicilastic rocks (2.4 g/cm^2 , following Owens et al.,
399 2018). We can determine the average sedimentation rate during the event using the observed thickness of
400 the OAE2 carbon isotope excursion in each core and the orbitally-tuned duration of OAE2 at the Global
401 Stratotype Section and Point in Pueblo, CO (Sageman et al., 2006; Meyers et al., 2012) of 540 kyr. A
402 constant sedimentation rate on the shelf during OAE2 is almost certainly an oversimplification but it is
403 sufficient for our purpose of comparing general trends between these cores. Using these values we find
404 organic carbon mass accumulation rates (OC MAR) during OAE2 average $0.05 \text{ g/cm}^2/\text{kyr}$ at Hope



405 Plantation, 0.04 g/cm²/kyr at Smith Elementary School, 0.06 g/cm²/kyr at Bass River, and 0.11 g/cm²/kyr
406 at Spinks. For comparison, the same method indicates OC MAR rates of 0.29 g/cm²/kyr at DSDP Site 603
407 and 2.84 g/cm²/kyr at Tarfaya (Owens et al., 2018). Owens et al. (2018) found an average OC MAR on
408 shelf sites during OAE2 of 0.11 g/cm²/kyr, which means the inner shelf sites on the east coast of North
409 America are below the global average during this event.

410 These data suggest a relationship with depth on the shelf and TOC deposition during OAE2. If
411 we arrange the sites by depth (Figure 7) we see the lowest average TOC values at Hope Plantation (0.63
412 wt%), the most proximal site; values are slightly higher at Smith Elementary (0.83 wt%) which appears to
413 represent an outer estuary or inner shelf environment, and higher still at Bass River (1.1 wt%) which was
414 inner to middle neritic (Miller et al., 2004). Estimates of organic carbon mass accumulation rates suggest
415 all three of these inner shelf sites are very similar, ranging from 0.4-0.6 g/cm² kyr. Average TOC is even
416 higher in the Spinks Core (1.4 wt%, or 0.11 g/cm² kyr), which represents inner to middle neritic depths
417 during the latter part of OAE2 (Lowery et al., 2017). This suggests the possibility of even higher values
418 on more distal parts of the shelf, and highlights the need for a true depth transect (as opposed to four cores
419 from three states) to better understand that variability and better constrain organic carbon burial in this
420 important environment during OAEs.

421 **6 Conclusions**

422 Calcareous nannoplankton biostratigraphy shows that positive carbon isotope excursions in two
423 cores on the Atlantic Coastal Plain in North Carolina are associated with the Cenomanian-Turonian
424 OAE2. C/N ratios in both cores indicate an increase in the proportion of land plants delivered to these
425 offshore sites during, indicating a strengthened hydrologic cycle causing increased terrigenous flux
426 beginning slightly before OAE2 and continuing through the whole event. This agrees with palynology-
427 based observations from the Bass River core ~500 km north (van Helmond et al., 2014). We therefore
428 conclude that these changes reflect increased precipitation and weathering across eastern North America
429 during OAE2, feeding nutrients onto the shelf and into the North Atlantic, and likely contributing to the



430 widespread black shale deposition in the deep basin. These cores are the second and third records of
431 OAE2, to our knowledge, on the coastal plain of eastern North America and, combined with the first
432 (Bowman and Bralower, 2005; van Helmond et al., 2014), show relatively low average TOC values (~0.6
433 - 1.1 wt%) on the inner shelf during this event, while suggesting a trend of increasing values with depth,
434 highlighting the need for more cores in this region from middle and outer shelf depths.

435 **Data Availability Statement**

436 Total organic carbon, total nitrogen, organic carbon isotope, geophysical and calcareous
437 nannofossil occurrence data are published (Self-Trail et al., 2021) and available for download as a USGS
438 Data Release at <https://doi.org/10.5066/P9V0U1NF>.

439 **Author Contribution**

440 CL and JS conceived of the study and sampled the cores. JS sat the wells in 2004 and 2005 and helped
441 describe the cores. CB conducted bulk organic carbon/nitrogen and organic carbon isotope measurements.
442 JS conducted calcareous nannoplankton biostratigraphy. CL supervised foraminifer analysis. CL prepared
443 the manuscript with contributions from JS and CB.

444 **Competing Interests Statement**

445 The authors declare that they have no conflicts of interest.

446 **Acknowledgements**

447 We are grateful to the drillers and personnel of the USGS for taking these cores, the staff of the North
448 Carolina Geological Survey for maintaining the cores and making them accessible for sampling, to Lara
449 Yagodzinski for her help sampling the cores, to Kate Gilbreath for her help preparing samples for
450 micropaleontological analysis, and to Ellen Seefelt for her assistance preparing samples for nannofossil
451 analysis and shipping material. Core box photographs courtesy USGS and NCGS. We acknowledge the
452 people, up to 200 at a time, who were held as slaves at Hope Plantation between 1748 and 1865. Any use



453 of trade, firm, or product names is for descriptive purposes only and does not imply endorsement by the
454 U.S. Government.

455 **References**

- 456 Aleman Gonzalez, W.B., Self-Trail, J.M., Harris, W.B., Moore, J.P., and Farrell, K.M. (2020). Depositional
457 sequence stratigraphy of Turonian to Santonian sediments, Cape Fear arch, North Carolina Coastal Plain,
458 USA. *Stratigraphy*, 17 (4), 293-314.
- 459 Applin, P.L., and Applin, E.R. (1944). Regional subsurface stratigraphy and structure of Florida and southern
460 Georgia. *American Association of Petroleum Geologists Bulletin*, 28 (12), 1673-1753.
- 461 Applin, P.L., and Applin, E.R. (1947). Regional subsurface stratigraphy, structure, and correlation of middle and
462 early Upper Cretaceous rocks in Alabama, Georgia, and north Florida. *U.S. Geological Survey Oil and Gas*
463 *Investigations Chart, OC- 26*, 3 sheets.
- 464 Applin, P.L., and Applin, E.R., (1967). The Gulf Series in the subsurface in northern Florida and southern Georgia.
465 *U.S. Geological Survey Professional Paper 524-G*, 40 pp.
- 466 Arthur, M. A., Schlanger, S. T., & Jenkyns, H. C. (1987). The Cenomanian-Turonian Oceanic Anoxic Event, II.
467 Palaeoceanographic controls on organic-matter production and preservation. *Geological Society, London,*
468 *Special Publications*, 26(1), 401-420.
- 469 Blättler, C. L., Jenkyns, H. C., Reynard, L. M., & Henderson, G. M. (2011). Significant increases in global
470 weathering during Oceanic Anoxic Events 1a and 2 indicated by calcium isotopes. *Earth and Planetary*
471 *Science Letters*, 309(1-2), 77-88.
- 472 Bown, P.R., and Young, J.R., 1998. Techniques. In: Bown, P.R., Ed., *Calcareous Nannofossil Biostratigraphy*, 16-
473 28. London: Kluwer Academic.
- 474 Burdige, D. J. (2007). Preservation of organic matter in marine sediments: controls, mechanisms, and an imbalance
475 in sediment organic carbon budgets?. *Chemical reviews*, 107(2), 467-485.
- 476 Burnett, J.A., 1998. Upper Cretaceous. In: Bown, P.R., Ed., *Calcareous Nannofossil Biostratigraphy*, 132-199.



- 477 Bowman, A. R., & Bralower, T. J. (2005). Paleooceanographic significance of high-resolution carbon isotope records
478 across the Cenomanian–Turonian boundary in the Western Interior and New Jersey coastal plain,
479 USA. *Marine Geology*, 217(3-4), 305-321.
- 480 Cooke, C.W. (1936). Geology of the Coastal Plain of South Carolina. *U.S. Geological Survey Bulletin* 867, 196pp.
- 481 Corbett, M.J., Watkins, D.K., and Pospichal, J.J., 2014. A quantitative analysis of calcareous nannofossil bioevents
482 of the Late Cretaceous (Late Cenomanian-Coniacian) Western Interior Seaway and their reliability in
483 established zonation schemes. *Marine Micropaleontology*, 109: 30-45.
- 484 Dorf, E., (1952). Critical analysis of Cretaceous stratigraphy and paleobotany of Atlantic Coastal Plain. *AAPG*
485 *Bulletin*, 36 (11), 2161-2184.
- 486 Erbacher, J., Friedrich, O., Wilson, P. A., Birch, H., & Mutterlose, J. (2005). Stable organic carbon isotope
487 stratigraphy across Oceanic Anoxic Event 2 of Demerara Rise, western tropical Atlantic. *Geochemistry,*
488 *Geophysics, Geosystems*, 6(6).
- 489 Friedrich, O., Norris, R. D., & Erbacher, J. (2012). Evolution of middle to Late Cretaceous oceans—a 55 my record
490 of Earth's temperature and carbon cycle. *Geology*, 40(2), 107-110.
- 491 Gale, A. S., and Christensen, W. K., (1996). Occurrence of the belemnite *Actinocamax plenus* in the Cenomanian of
492 SE France and its significance. In *Bulletin of the Geological Society of Denmark*, 43(1), 68-77.
- 493 Gale, A. (2019). Correlation, age and significance of Turonian Chalk hardgrounds in southern England and northern
494 France: The roles of tectonics, eustasy, erosion and condensation. *Cretaceous Research*, 103, 104164.
- 495 Gohn, G. S. (1992). Revised nomenclature, definitions, and correlations for the Cretaceous formations in USGS-
496 Clubhouse Crossroads# 1, Dorchester County, South Carolina. *U.S. Geological Survey Professional Paper*
497 *1518*, 39 pp.
- 498 Gohn, G.S. 1995. Ostracode biostratigraphy of the Upper Cretaceous marine sediments in the New Jersey Coastal
499 Plain. In: Baker, J.E.B. (Ed.), Contributions to the paleontology of New Jersey. Geological Association of
500 New Jersey Annual Field Conference, 12th Annual Meeting, Wayne, NJ, Oct. 27-28, 1995, v. 12, p. 87-
501 101.Gale



- 502 Hasegawa, T., Crampton, J. S., Schiøler, P., Field, B., Fukushi, K., & Kakizaki, Y. (2013). Carbon isotope
503 stratigraphy and depositional oxia through Cenomanian/Turonian boundary sequences (Upper Cretaceous)
504 in New Zealand. *Cretaceous research*, 40, 61-80.
- 505 Hattner, J.G., and Wise, S.W., Jr., (1980). Upper Cretaceous calcareous nannofossil biostratigraphy of South
506 Carolina. *South Carolina Geology*, 24(2), 41-117.
- 507 Hazel, J.E., Bybell, L.M., Christopher, R.A., Frederiksen, N.O., May, F.E., McLean, D.M., Poore, R.Z., Smith,
508 C.C., Sohl, N.F., Valentine, P.C., and Witmer, R.J., (1977). Biostratigraphy of the deep corehole
509 (Clubhouse Crossroads corehole 1) near Charleston, South Carolina, in Rankin, D.W., (Ed.), Studies related
510 to the Charleston, South Carolina earthquake of 1886—A preliminary report. *U.S. Geological Survey*
511 *Professional Paper 1028*, p. 71-89.
- 512 Heron, S.D., Jr. (1958). History of terminology and correlations of the basal Cretaceous formations of the
513 Carolinas. *South Carolina Division of Geology Bulletin 2*, p. 77-88.
- 514 Jarvis, I., Lignum, J. S., Gröcke, D. R., Jenkyns, H. C., & Pearce, M. A. (2011). Black shale deposition, atmospheric
515 CO₂ drawdown, and cooling during the Cenomanian-Turonian Oceanic Anoxic
516 Event. *Paleoceanography*, 26(3).
- 517 Jenkyns, H. C. (2010). Geochemistry of oceanic anoxic events. *Geochemistry, Geophysics, Geosystems*, 11(3).
- 518 Kennedy, W. J., Walaszczyk, I., & Cobban, W. A. (2005). The global boundary stratotype section and point for the
519 base of the Turonian stage of the Cretaceous: Pueblo, Colorado, USA. *Episodes*, 28(2), 93-104.
- 520 Kolonic, S., Wagner, T., Forster, A., Sinninghe Damsté, J. S., Walsworth-Bell, B., Erba, E., Turgeon, S., Brumsack,
521 H.J., Chellai, E.H., Tsikos, H., & Kuhnt, W. (2005). Black shale deposition on the northwest African Shelf
522 during the Cenomanian/Turonian oceanic anoxic event: Climate coupling and global organic carbon
523 burial. *Paleoceanography*, 20(1).
- 524 Kuypers, M. M., Lourens, L. J., Rijpstra, W. I. C., Pancost, R. D., Nijenhuis, I. A., & Damsté, J. S. S. (2004).
525 Orbital forcing of organic carbon burial in the proto-North Atlantic during oceanic anoxic event 2. *Earth*
526 *and Planetary Science Letters*, 228(3-4), 465-482.



- 527 Leckie, R. M., Yuretich, R. F., West, O. L., Finkelstein, D., & Schmidt, M. (1998). Paleooceanography of the
528 southwestern Western Interior Sea during the time of the Cenomanian-Turonian boundary (Late
529 Cretaceous).
- 530 Leckie, R. M., Bralower, T. J., & Cashman, R. (2002). Oceanic anoxic events and plankton evolution: Biotic
531 response to tectonic forcing during the mid-Cretaceous. *Paleoceanography*, 17(3), 13-1.
- 532 Lowery, C. M., Cunningham, R., Barrie, C. D., Bralower, T., & Snedden, J. W. (2017). The northern Gulf of
533 Mexico during OAE2 and the relationship between water depth and black shale
534 development. *Paleoceanography*, 32(12), 1316-1335.
- 535 McAnena, A., Flögel, S., Hofmann, P., Herrle, J.O., Griesand, A., Pross, J., Talbot, H.M., Rethemeyer, J., Wallmann,
536 K., & Wagner, T., 2013. Atlantic cooling associated with a marine biotic crisis during the mid-Cretaceous
537 period. *Nature Geoscience* 6, no. 7 (2013): 558-561.
- 538 Meyers, P. A. (1994). Preservation of elemental and isotopic source identification of sedimentary organic matter.
539 *Chemical Geology* 114, 289-302.
- 540 Meyers, P. A. (1997). Organic geochemical proxies of paleoceanographic, paleolimnologic, and paleoclimatic
541 processes. *Organic geochemistry*, 27(5-6), 213-250.
- 542 Meyers, P. A. (2003). Applications of organic geochemistry to paleolimnological reconstructions: a summary of
543 examples from the Laurentian Great Lakes. *Organic geochemistry*, 34(2), 261-289.
- 544 Meyers, S. R., Siewert, S. E., Singer, B. S., Sageman, B. B., Condon, D. J., Obradovich, J. D., Jicha, B.R., &
545 Sawyer, D. A. (2012). Intercalibration of radioisotopic and astrochronologic time scales for the
546 Cenomanian-Turonian boundary interval, Western Interior Basin, USA. *Geology*, 40(1), 7-10.
- 547 Miller, K.G., Sugarman, P.J., Browning, J.V., et al., 1998. Bass River site. *Proceedings of the Ocean Drilling
548 Program, Initial Reports*, v. 174AX, p. 1-39.
- 549 Miller, K.G., Sugarman, P.J., Browning, J.V., Kominz, M.A., Olsson, R.K., Feigenson, M.D., and Hernandez, J.C.,
550 2004. Upper Cretaceous sequences and sea-level history, New Jersey Coastal Plain. *GSA Bulletin*, 116:
551 368-393.



- 552 Monteiro, F. M., Pancost, R. D., Ridgwell, A., & Donnadieu, Y. (2012). Nutrients as the dominant control on the
553 spread of anoxia and euxinia across the Cenomanian-Turonian oceanic anoxic event (OAE2): Model-data
554 comparison. *Paleoceanography*, 27(4).
- 555 O'Connor, L. K., Jenkyns, H. C., Robinson, S. A., Remmelzwaal, S. R., Batenburg, S. J., Parkinson, I. J., & Gale, A.
556 S. (2020). A Re-evaluation of the Plenus Cold Event, and the Links Between CO₂, Temperature, and
557 Seawater Chemistry During OAE 2. *Paleoceanography and Paleoclimatology*, 35(4), e2019PA003631.
- 558 Ostrander, C. M., Owens, J. D., & Nielsen, S. G. (2017). Constraining the rate of oceanic deoxygenation leading up
559 to a Cretaceous Oceanic Anoxic Event (OAE-2:~ 94 Ma). *Science advances*, 3(8), e1701020.
- 560 Owens, J. D., Lyons, T. W., Hardisty, D. S., Lowery, C. M., Lu, Z., Lee, B., & Jenkyns, H. C. (2017). Patterns of
561 local and global redox variability during the Cenomanian–Turonian Boundary Event (Oceanic Anoxic
562 Event 2) recorded in carbonates and shales from central Italy. *Sedimentology*, 64(1), 168-185.
- 563 Owens, J. D., Lyons, T. W., & Lowery, C. M. (2018). Quantifying the missing sink for global organic carbon burial
564 during a Cretaceous oceanic anoxic event. *Earth and Planetary Science Letters*, 499, 83-94.
- 565 Petters, S.W., 1976. Upper Cretaceous subsurface stratigraphy of Atlantic Coastal Plain of New Jersey. *AAPG*
566 *Bulletin*, v. 60, n. 1, p. 87-107.
- 567 Petters, S.W., 1977. Upper Cretaceous planktonic foraminifera from the subsurface of the Atlantic Coastal Plain of
568 New Jersey. *Journal of Foraminiferal Research*, 7: 165-187.
- 569 Pogge Von Strandmann, P. A., Jenkyns, H. C., & Woodfine, R. G. (2013). Lithium isotope evidence for enhanced
570 weathering during Oceanic Anoxic Event 2. *Nature Geoscience*, 6(8), 668-672. Prah et al., 1980
- 571 Pratt, L. M., & Threlkeld, C. N. (1984). Stratigraphic significance of ¹³C/¹²C ratios in mid-Cretaceous rocks of the
572 Western Interior, USA.
- 573 Richards, H.G. (1945). Subsurface stratigraphy of Atlantic Coastal Plain between New Jersey and Georgia.
574 *American Association of Petroleum Geologists Bulletin*, 29 (7), 885-955.
- 575 Sageman, B. B., Meyers, S. R., & Arthur, M. A. (2006). Orbital time scale and new C-isotope record for
576 Cenomanian-Turonian boundary stratotype. *Geology*, 34(2), 125-128.



- 577 Schlanger, S. O., & Jenkyns, H. C. (1976). Cretaceous oceanic anoxic events: causes and consequences. *Geologie en*
578 *mijnbouw*, 55(3-4).
- 579 Scholle, P. A., & Arthur, M. A. (1980). Carbon isotope fluctuations in Cretaceous pelagic limestones: potential
580 stratigraphic and petroleum exploration tool. *AAPG Bulletin*, 64(1), 67-87.
- 581 Seefelt, E.L., Self-Trail, J.M., and Schultz, A.P., 2015. Comparison of three preservation techniques for slowing
582 dissolution of calcareous nannofossils in organic-rich sediments. *Micropaleontology*, v. 61, n. 3, p. 149-
583 164.
- 584 Self-Trail, J.M., and Bybell, L.M., 1995. Cretaceous and Paleogene calcareous nannofossil biostratigraphy of New
585 Jersey. In: Baker, J.E.B. (Ed.), Contributions to the paleontology of New Jersey. Geological Association
586 of New Jersey Annual Field Conference, 12th Annual Meeting, Wayne, NJ, Oct. 27-28, 1995, v. 12, p. 102-
587 139.
- 588 Self-Trail, J.M., and Seefelt, E.L., 2005. Rapid dissolution of calcareous nannofossils: a case study from freshly
589 cored sediments of the south-eastern Atlantic Coastal Plain. *Journal of Nannoplankton Research*, v. 27, n.
590 20, p. 149-157.
- 591 Self-Trail, J.M., Barrie, C., and Lowery, C.M., 2021. USGS Data Release.
- 592 Shamrock, J.L., Munoz, E.J., and Carter, J.H., 2015. An improved sample preparation technique for calcareous
593 nannofossils in organic-rich mudstones. *Journal of Nannoplankton Research*, v. 35, n. 2, 101-110.
- 594 Shamrock, J.L., and Self-Trail, J.M., 2016. Quantification of a pretreatment procedure for organic-rich calcareous
595 nannofossil samples. *Journal of Nannoplankton Research*, v. 36, n. 1, 65-75.
- 596 Sikora, P.J., and Olsson, R.K., 1991. A paleoslope model of late Albian to early Turonian foraminifera of the
597 western Atlantic margin and North Atlantic basin. *Marine Micropaleontology*, v. 18, p. 25-72.
- 598 Sissinghi, W., 1977. Biostratigraphy of Cretaceous calcareous nannoplankton. *Geologie en Mijnbouw*, 56: 37-65.
- 599 Slattery, J. S., Cobban, W. A., McKinney, K. C., Harries, P. J., & Sandness, A. L. (2015). Early Cretaceous to
600 Paleocene paleogeography of the Western Interior Seaway: the interaction of eustasy and
601 tectonism. *Wyoming Geological Association Guidebook*, 2015, 22-60.



- 602 Snedden, J. W., Virdell, J., Whiteaker, T. L., & Ganey-Curry, P. (2015). A basin-scale perspective on Cenomanian-
603 Turonian (Cretaceous) depositional systems, greater Gulf of Mexico (USA). *Interpretation*, 4(1), SC1-
604 SC22.
- 605 Snow, L. J., Duncan, R. A., & Bralower, T. J. (2005). Trace element abundances in the Rock Canyon Anticline,
606 Pueblo, Colorado, marine sedimentary section and their relationship to Caribbean plateau construction and
607 oxygen anoxic event 2. *Paleoceanography*, 20(3).
- 608 Spangler, W. B. (1950). Subsurface geology of Atlantic coastal plain of North Carolina. *AAPG Bulletin*, 34(1), 100-
609 132.
- 610 Sohl, N. F., & Owens, J. P. (1991). Cretaceous stratigraphy of the Carolina coastal plain. *The geology of the*
611 *Carolinas*, 191-220.
- 612 Stephenson, L.W., 1912. The Cretaceous formations. In: Clark, W.B., Miller, B.L., Stephenson, L.W., Johnson,
613 B.L., and Parker, H.N., Eds. The Coastal Plain of North Carolina. *North Carolina Geologic and Economic*
614 *Survey*, 3: 73-171.
- 615 Tarduno, J. A., Sliter, W. V., Kroenke, L., Leckie, M., Mayer, H., Mahoney, J. J., Musgrave, R., Sotery, M., &
616 Winterer, E. L. (1991). Rapid formation of Ontong Java Plateau by Aptian mantle plume
617 volcanism. *Science*, 254(5030), 399-403.
- 618 Thornburg, J., 2008. “Temporal variations in the paleopedology and paleoclimatology of the Early
619 Cretaceous Potomac Group, Hope Plantation core, Bertie County, North Carolina”. Unpublished
620 Masters Thesis, Temple University, Pennsylvania.
- 621 Tibert, N. E., & Leckie, R. M. (2004). High-resolution estuarine sea level cycles from the Late Cretaceous:
622 Amplitude constraints using agglutinated foraminifera. *The Journal of Foraminiferal Research*, 34(2), 130-
623 143.
- 624 Tsikos, H., Jenkyns, H. C., Walsworth-Bell, B., Petrizzo, M. R., Forster, A., Kolonic, S., ... & Damsté, J. S. (2004).
625 Carbon-isotope stratigraphy recorded by the Cenomanian–Turonian Oceanic Anoxic Event: correlation and
626 implications based on three key localities. *Journal of the Geological Society*, 161(4), 711-719.



- 627 Turgeon, S. C., & Creaser, R. A. (2008). Cretaceous oceanic anoxic event 2 triggered by a massive magmatic
628 episode. *Nature*, 454(7202), 323-326.
- 629 Valentine, P. C. (1982). *Upper Cretaceous subsurface stratigraphy and structure of coastal Georgia and South*
630 *Carolina* (No. 1222). U.S. Geological Survey Professional Paper 1222, 33 p.
- 631 Valentine, P.C., (1984). Turonian (Eaglefordian) stratigraphy of the Atlantic Coastal Plain and Texas. *U.S.*
632 *Geological Survey Professional Paper 1315*, 21pp.
- 633 van Helmond, N. A., Sluijs, A., Reichart, G. J., Damsté, J. S. S., Slomp, C. P., & Brinkhuis, H. (2014). A perturbed
634 hydrological cycle during Oceanic Anoxic Event 2. *Geology*, 42(2), 123-126.
- 635 van Helmond, N. A., Sluijs, A., Sinninghe Damsté, J. S., Reichart, G. J., Voigt, S., Erbacher, J., ... & Brinkhuis, H.
636 (2015). Freshwater discharge controlled deposition of Cenomanian–Turonian black shales on the NW
637 European epicontinental shelf (Wunstorf, northern Germany). *Climate of the Past*, 11, 495-508.
- 638 Weems, R. E., Seefelt, E. L., Wrege, B. M., Self-Trail, J. M., Prowell, D. C., Durand, C., Cobbs, E.F., & McKinney,
639 K. C. (2007). Preliminary physical stratigraphy and geophysical data of the USGS Hope Plantation Core
640 (BE-110), Bertie County, North Carolina. *US Geological Survey Open-File Report, 1251*, 1-163.
- 641 Weems, R. E., Self-Trail, J. M., and Edwards, L. E., 2019. Cross Section of the North Carolina Coastal Plain from
642 Enfield through Cape Hatteras. *US Geological Survey Open-File Report, 2019-1145*.
- 643 Whitechurch, H., Montigny, R., Sevigny, J., Storey, M., & Salters, V. (1992). K-Ar and ⁴⁰Ar-³⁹Ar ages of central
644 Kerguelen Plateau basalts. In *Proc. Ocean Drill. Program Sci. Results* (Vol. 120, pp. 71-77).
- 645 Woolf, K. S. (2012). Regional character of the Lower Tuscaloosa Formation depositional systems and trends in
646 reservoir quality. PhD Thesis.
- 647 Zarra, L. (1989). *Sequence stratigraphy and foraminiferal biostratigraphy for selected wells in the Albemarle*
648 *Embayment, North Carolina*. North Carolina Geological Survey Open File Report 89-5. 52 p.